Spheroidal Galaxies/QSOs Connection

Luigi Danese[1], Gian Luigi Granato[2], Laura Silva[3], Manuela Magliocchetti[1], and Gianfranco De Zotti[2]

[1] SISSA/ISAS, Via Beirut 2–4, I-34014 Trieste, Italy
[2] Osservatorio Astronomico di Padova, Vicolo dell'Osservatorio 5, I-35122 Padova, Italy
[3] Osservatorio Astronomico di Trieste, Via Tiepolo 11, I-34131 Trieste, Italy

Abstract. In view of the extensive evidence of a tight inter-relationship between spheroidal galaxies (and galactic bulges) and massive black holes hosted at their centers, a consistent model must deal jointly with the evolution of the two components. We describe one viable model, which successfully accounts for the local luminosity function of spheroidal galaxies, their photometric and chemical properties, deep galaxy counts in different wavebands, including those in the (sub)-mm region which proved to be critical for current semi-analytic models stemming from the standard hierarchical clustering picture, clustering properties of SCUBA galaxies, of EROs, and of LBGs, as well as for the local mass function of massive black holes and for quasar evolution. Predictions that can be tested by surveys carried out by SIRTF are presented.

1 Introduction

The hierarchical clustering model with a scale invariant spectrum of density perturbations in a Cold Dark Matter (CDM) dominated universe has proven to be remarkably successful in matching the observed large-scale structure as well as a broad variety of properties of galaxies of different morphological types (e.g. [6,18]). However, serious shortcomings of this scenario have also become evident in recent years. The critical point can be traced back to the relatively large amount of power on small scales predicted by this model which would imply far more dwarf galaxies or substructure clumps within galactic and cluster mass halos than are observed (the so-called "small-scale crisis" ([20,54,24,37]), unless star formation in small objects is strongly suppressed (or the small scale power is reduced by modifying the standard model).

At the other extreme of the galaxy mass function we have another strong discrepancy with model predictions, that we might call "the massive galaxy crisis": even the best semi-analytic models ([18,9]) hinging upon the standard picture for structure formation in the framework of the hierarchical clustering paradigm, fall short by a substantial factor (up to about 10) to account for the (sub)-mm (SCUBA and MAMBO) counts of galaxies, most of which are probably massive objects undergoing a very intense star-burst (with star formation rates $\sim 1000\,\mathrm{M}_\odot\,\mathrm{yr}^{-1}$) at $z > 2$ (see, e.g. [10]). Recent optical data confirm that most massive ellipticals were already in place and (almost) passively evolving up to $z \simeq 1$–1.5, implying that they were fully assembled by $z \sim 2.5$, although the issue is still somewhat controversial ([47,13,8,30,48,5,23,31]). These data are

more consistent with the traditional "monolithic" approach whereby giant ellipticals formed most of their stars in a single gigantic starburst at substantial redshifts, and underwent essentially passive evolution thereafter.

On the contrary, in the canonical hierarchical clustering paradigm the smallest objects collapse first and most star formation occurs, at relatively low rates, within relatively small proto-galaxies, that later merged to form larger galaxies. Thus, the expected number of galaxies with very intense star formation is far less than detected in SCUBA and MAMBO surveys and the surface density of massive evolved ellipticals at $z \gtrsim 1$ is also smaller than observed. The "monolithic" approach, however, is inadequate to the extent that it cannot be fitted in a consistent scenario for structure formation from primordial density fluctuations.

2 Relationships between quasar and galaxy evolution

The above difficulties, affecting even the best current recipes, may indicate that new ingredients need to be taken into account. A key new ingredient may be the mutual feedback between formation and evolution of spheroidal galaxies and of active nuclei residing at their centers ([25,29,21,59,14–16,33–35]). In this framework, [19] elaborated the following scheme (see also [11,53,36]):

- Feed-back effects, from supernova explosions and from active nuclei (note that supernova feedback alone falls short of solving the dearth of dwarf galaxies, [27], but photo-ionization by the UV background re-ionizing the inter-galactic medium (IGM) could do the job [54]) delay the collapse of baryons in smaller clumps while large ellipticals form their stars as soon as their potential wells are in place; *the canonical hierarchical CDM scheme – small clumps collapse first – is therefore reversed for baryons.*
- Large spheroidal galaxies therefore undergo a phase of high (sub)-mm luminosity.
- At the same time, the central black-hole (BH) grows by accretion and the quasar luminosity increases; when it reaches a high enough value, its action (ionization and heating of the gas) stops the star formation and eventually expels the residual gas. This explains the observed correlation between BH and host spheroidal masses (see [53,12]). The same mechanism distributes in the IGM a substantial fraction of metals and may pre-heat the IGM. The onset of quasar activity (and the corresponding squelching of star formation) occurs earlier for more massive objects. The duration of the star-burst increases with decreasing mass from ~ 0.5 to $\sim 2\,\mathrm{Gyr}$.
- This implies that the star-formation activity of the most massive galaxies quickly declines for $z \lesssim 3$, i.e. the redshift distribution of SCUBA/MAMBO galaxies should peak at $z \gtrsim 3$, just before quasars reach their maximum luminosity (at $z \simeq 2.5$). This:
  - explains why very luminous quasars are more easily detected at (sub)-mm wavelengths for $z \gtrsim 2.5$ [39]. The latter authors argue that a large

fraction of the observed (sub)-mm emission is powered by a starburst, as expected from this model
  - implies an extremely steep (essentially exponential) decline of (sub)-mm counts at bright fluxes, as indicated by recent data.
- A "quasar phase" follows, lasting 10^7–10^8 yrs.
- A long phase of passive evolution of galaxies ensues, with their colors becoming rapidly very red [Extremely Red Object (ERO) phase].
- Intermediate- and low-mass spheroids have lower Star Formation Rates and less extreme optical depths. They show up as Lyman-Break Galaxies (LBGs).
- Therefore, in this scenario, large ellipticals evolve essentially as in the "monolithic" scenario, yet in the framework of the standard hierarchical clustering picture.

The various aspects and implications of this compound scheme have been addressed by our group in a series of papers. [51] estimated the mass function of quiescent BHs at the centers of local galaxies. They found a dichotomy between large and small BHs: the former are hosted in elliptical galaxies and tend to be not obscured, while the latter, found in the bulges of spiral galaxies, can be reactivated by interactions and are frequently obscured. Their results are consistent with the high luminosity quasar activity occurring as a single short-lived event at relatively high redshift with luminosity close to the Eddington limit. Later, lower luminosity, nuclear activity may be due to re-activation of the central BH, due, e.g., to interactions. [36] analyzed the evolution of the quasar luminosity function in the framework of a model in which the spheroidal galaxies (and bulges of later-type galaxies) and the BHs at their centers form and evolve in parallel. Adopting the standard [46] formation rate of dark matter halos, they found that consistency with the data is achieved if, and only if, BHs in bigger galactic halos form earlier. In other words, the interval between the onset of star formation and the peak of quasar luminosity is shorter for the more massive objects. Some of the other, most recent, results are briefly described in the next section.

3 Some recent results and predictions

3.1 Counts at (sub)-mm wavelengths

The (sub)-mm counts are expected to be very steep because of the combined effect of the strong cosmological evolution of dust emission in spheroidal galaxies and of the strongly negative K-correction (the dust emission spectrum steeply rises with increasing frequency). The model by [19] has extreme properties in this respect: above several mJy its 850 μm counts reflect the high-mass exponential decline of the mass function of dark halos. In this model, SCUBA/MAMBO galaxies correspond to the phase when massive spheroids formed most of their stars at $z \gtrsim 2.5$; such objects essentially disappear at lower redshifts. On the contrary, the counts predicted by alternative models (which are essentially phenomenological [3,55,50,41,56]), while steep, still have a power law shape, and the redshift distribution has an extensive low-z tail.

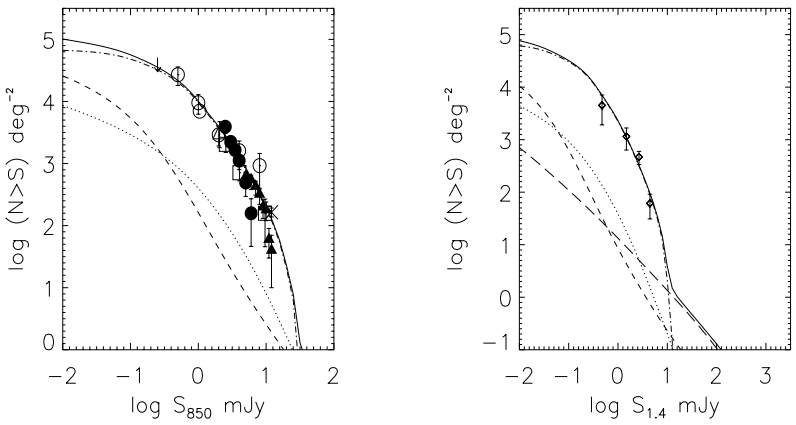

Fig. 1. Integral source counts at 850 μm (left panel) and at 1.4 mm (right panel) predicted by the model by [19] compared with observations. The dotted, dashed and dot-dashed lines show the contributions of starburst, spiral, and forming elliptical galaxies, respectively. The long-dashed line (shown only at 1.4 mm) gives the counts of radio sources, after [57]. The solid line shows the total counts. References for the data points can be found in [44]

As illustrated by Fig. 1, the recent relatively large area surveys [52,4] are indeed suggestive of an exponential decline of the 850 μm counts above several mJy. Further evidence in this direction comes from MAMBO surveys at 1.2 mm [2]; see [44]).

3.2 Lensing effects on (sub)-mm counts

A direct consequence of the extreme steepness of the (sub)-mm counts predicted by this model is that their bright tail is strongly affected by gravitational lensing [43,44]. In fact, although the probability of strong lensing is very small, it has a power-law tail ($p(A) \propto A^{-3}$) extending up to large values of the magnification A. Thus, if counts are steep enough, the fraction of lensed sources at bright fluxes may be large.

[43] and [44] find that, according to the model by [19], essentially all proto-spheroidal galaxies brighter than $S_{850\mu\mathrm{m}} \simeq 60$–$70$ mJy are gravitationally lensed. Allowing for the other populations of sources contributing to the bright mm/sub-mm counts, they find that the fraction of gravitationally lensed sources may be $\simeq 40\%$ at fluxes slightly below $S_{850\mu\mathrm{m}} = 100$ mJy. If so, large area surveys such as those to be carried out by PLANCK/HFI or by forthcoming balloon experiments like BLAST and ELISA will probe the large scale distribution of the peaks of the primordial density field. For comparison, the maximum fraction of lensed sources predicted by current phenomenological models is $\lesssim 5\%$.

3.3 Clustering of SCUBA/MAMBO galaxies

Since, in the above scheme, SCUBA galaxies correspond to the rare, massive density peaks at high-z, they are expected to be highly biased tracers of the dark matter distribution, and therefore to be strongly clustered. The recent analyses by [28] and [44] have shown that the implied angular correlation function is indeed consistent with the results by [17] on the clustering of LBGs, and by [52] and [40] on clustering of SCUBA galaxies. The estimated $w(\theta)$ for bright SCUBA galaxies [52] and for EROs [7] indicate dark halo masses $10^{13}\,\mathrm{M}_{\odot}$ for these sources; the $w(\theta)$ for LBGs [17] indicate typical masses at least 10 times lower (see also [38]).

3.4 Chemical and photometric evolution

The problem has been addressed by [49]. The short duration of the star-burst in spheroidal galaxies, and its occurrence at $z \gtrsim 3$, assumed by the model, are consistent with the supra-solar Mg/Fe ratio in ellipticals, with the tightness of their fundamental plane and of their color–σ relation. But the model also compares successfully with a broad variety of detailed observational data: the correlation between the abundances of Fe and those of "enhanced" elements (C, N, O, Ne, Mg, Si, S), the correlation between Fe and Mg_2, the template Spectral Energy Distribution of local ellipticals, the color $(V-K)$-magnitude (M_V) and the $(J-K)$–$(V-K)$ relations. The key ingredients allowing to match the observational data, and in particular the relationships among abundances of the various elements are, on one side, the decrease of the duration of the star-burst with increasing galactic mass, and, on the other side, the fact that the effect of stellar feedback is higher in less massive objects, so that the amount of material enriched by SNII that can be retained is lower. The main difference with the majority of previous chemical evolution models is that star formation is stopped not by supernova-driven winds (which also fall short of providing enough preheating of the proto-cluster medium, [58,1,26]), but by the energy injected by the active nucleus.

Note that this model also accounts for the roughly solar, or supra-solar, metallicity of the quasar broad-line regions and of supra-solar N/C and Fe/α ratios in the more luminous objects observed out to $z > 4$ [22] and even up to $z \sim 6$ [42]. This implies that the medium must have been chemically enriched before the quasars became observable and on short timescales ($\leq 1\,\mathrm{Gyr}$, at least at the highest redshifts).

Another interesting implication of the model, also discussed by [49], is the dependence of the ratio $M_{\mathrm{darkmatter}}/M_{\mathrm{stars}}$ on M_{stars}. This ratio has a minimum value $\simeq 20$ for $M_{\mathrm{stars}} \simeq 10^{10}$–$10^{11}\,\mathrm{M}_{\odot}$, in good agreement with the results by [32], and increases at smaller masses (in keeping with the findings by [45]) due to the increasing fraction of gas expelled by supernova feedback, as well as at higher masses, due to the increase of the cooling time of the gas in the outer regions of the galactic halo.

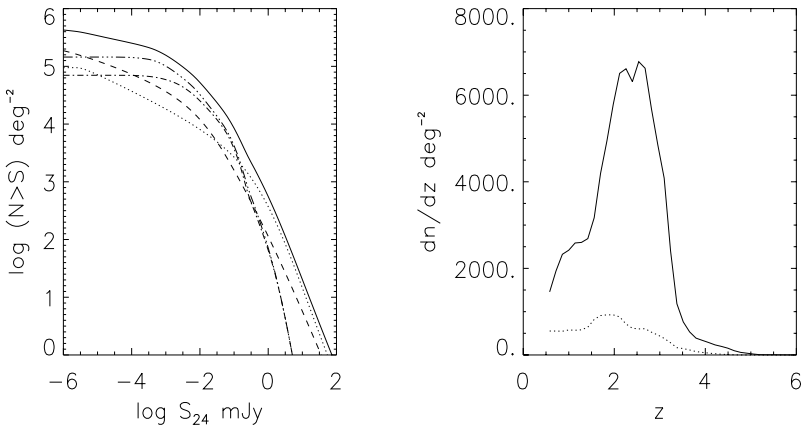

Fig. 2. Integral source counts (left-hand panel) and redshift distribution (right-hand panel) for a flux limit of 30μJy (right panel) at 24 μm predicted by the model by [19]. In the left-hand panel, the dotted, dashed and dot-dashed lines show the contributions of starburst, spiral, and forming elliptical galaxies, respectively, while the three-dots/dashed line shows the total counts of ellipticals, including also those where the star-formation has ended. In the right-hand panel, the solid and the dotted lines show the redshift distributions of ellipticals during and after the star-formation phase, respectively

3.5 Predictions for SIRTF surveys

SIRTF surveys have the potential of providing further tests of the model. In particular, the GOODS (http://www.stsci.edu/science/goods) 24 μm survey should reach the confusion limit at 30–100 μJy. According to the model, about 50% of the detected galaxies should be spheroidal galaxies forming their stars at $z \gtrsim 2$. About 400–600 such objects are expected over an area of 0.1 square degree (see Fig. 2). Their redshift distribution is predicted to peak at z slightly above 2, with a significant tail extending up to $z \gtrsim 3$.

Acknowledgements. We benefited from many helpful exchanges with C. Baccigalupi, F. Matteucci, F. Perrotta, D. Romano. Work supported in part by ASI and MIUR.

References

1. M.L. Balogh, F. Pearce, R.G. Bower, S. Kay: MNRAS **326**, 1228 (2001)
2. F. Bertoldi, K.M. Menten, E. Kreysa, C.L. Carilli, F. Owen: in *Cold Gas and Dust at High Redshift*, ed. by D.J. Wilner, Highlights of Astronomy, Vol. 12 (2000)
3. A.W. Blain, A. Jameson et al.: MNRAS **309**, 715 (1999)
4. C. Borys, S. Chapman, M. Halpern, D. Scott D.: MNRAS, submitted (2001)
5. J.G. Cohen: AJ **121**, 2895 (2001)
6. S. Cole, C.G. Lacey, C.M. Baugh, M. Carlton, C.S. Frenk: MNRAS **319**, 168 (2000)
7. E. Daddi, A. Cimatti, et al.: A&A **361**, 535 (2000)

8. E. Daddi, A. Cimatti, A. Renzini: A&A **362**, L45 (2000)
9. J.E.G. Devriendt, B. Guiderdoni: A&A **363**, 851 (2000)
10. J.S. Dunlop: New Astr. Rev. **45**, 609 (2001)
11. S.A. Eales, M.G. Edmunds: MNRAS **280**, 1167 (1996)
12. A.C. Fabian: MNRAS **308**, L39 (1999)
13. H.C. Ferguson, M. Dickinson, R. Williams: 2000, ARA&A **38**, 667 (2000)
14. L. Ferrarese, D. Merritt: ApJ **539**, L9 (2000)
15. K. Gebhardt, R. Bender et al.: ApJ **539**, L13 (2000)
16. K. Gebhardt, J. Kormendy et al.: ApJ **543**, L5 (2000)
17. M. Giavalisco, C.C. Steidel et al.: ApJ **503**, 543 (1998)
18. G.L. Granato, C.G. Lacey et al.: ApJ **542**, 710 (2000)
19. G.L. Granato, L. Silva et al.: MNRAS **324**, 757 (2001)
20. Z. Haiman, R. Barkana, J.P. Ostriker: in *Proc. 20th Texas Symp.* (2001)
21. P.B. Hall, R.F. Green: ApJ **507**, 558 (1998)
22. F. Hamann, G. Ferland: ARA&A **37**, 487 (1999)
23. M. Im, S.M. Faber et al.: AJ, **122**, 750 (2001)
24. M. Kamionkowski, A.R. Liddle: Phys. Rev. Lett. **84**, 4525 (2000)
25. J. Kormendy, D. Richstone: ARA&A **33**, 581 (1995)
26. A.V. Kravtsov, G. Yepes: MNRAS **318**, 227 (2000)
27. M.-M. MacLow, A. Ferrara: ApJ **513**, 142 (1999)
28. M. Magliocchetti, L. Moscardini at al.: MNRAS, **325**, 1553 (2001)
29. J. Magorrian, S. Tremaine et al.: AJ **115**, 2295 (1998)
30. P. Martini: AJ **121**, 2301 (2001)
31. P.J. McCarthy, R.G. Carlberg et al.: ApJ **560**, L131 (2001)
32. T.A. McKay, E.S. Sheldon, et al.: ApJ, submitted, astro-ph/0108013 (2001)
33. R.J. McLure, J.S. Dunlop: MNRAS **327**, 199 (2001)
34. D. Merritt, L. Ferrarese: MNRAS **320**, L30 (2001)
35. D. Merritt, L. Ferrarese: ApJ **547**, 140 (2001)
36. P. Monaco, P. Salucci, L. Danese: MNRAS **311** 279 (2001)
37. B. Moore, S. Ghigna et al.: ApJ, **524**, L19 (1999)
38. L.A. Moustakas, R.S. Somerville: ApJ, submitted, astro-ph/0110584 (2001)
39. A. Omont, P. Cox et al.: &A **374**, 371 (2001)
40. J.A. Peacock, M. Rowan-Robinson et al.: MNRAS **318**, 535 (2000)
41. C.P. Pearson, H. Matsuhara et al.: MNRAS **324**, 999 (2001)
42. L. Pentericci, X. Fan et al.: AJ, submitted, astro-ph/0112075 (2001)
43. F. Perrotta, C. Baccigalupi et al.: MNRAS **329**, 445 (2002)
44. F. Perrotta, M. Magliocchetti et al.: MNRAS, submitted, astro-ph/0111239 (2001)
45. M. Persic, P. Salucci, F. Stel: MNRAS **281**, 27 (1996)
46. W.H. Press, P. Schechter: ApJ **187**, 425 (1974)
47. A. Renzini, A. Cimatti: 1999, in *The Hy-Redshift Universe: Galaxy Formation and Evolution at High Redshift*, ASP conf. ser. **193**, p. 312 (1999)
48. G. Rodighiero, A. Franceschini, G. Fasano: MNRAS **324**, 491 (2001)
49. D. Romano, L. Silva, F. Matteucci, L. Danese: preprint (2001)
50. M. Rowan-Robinson: ApJ **549** 745 (2001)
51. P. Salucci, E. Szuszkiewicz, P. Monaco, L. Danese, L.: MNRAS **307** 637 (1999)
52. S.E. Scott, M. Fox et al.: MNRAS, submitted, astro-ph/0107446 (2001)
53. J. Silk, M.J. Rees: A&A **331**, L1 (1998)
54. R.S. Somerville: ApJL, submitted, astro-ph/0107507 (2001)
55. J.C. Tan, J. Silk, C. Balland: ApJ **522**, 579 (1999)
56. T.T. Takeuchi, R. Kawabe et al.: PASP **113**, 586 (2001)
57. L. Toffolatti, F. Argüeso Gómez et al.: MNRAS **297**, 117 (1998)
58. P. Valageas, J. Silk: A&A **350**, 725 (1999)
59. R.P. van der Marel: AJ **117**, 744 (1999)